

Measurement of DNA Morphological Parameters at Highly Entangled Regime on Surfaces

Annalisa Calò, Pablo Stoliar, Eva Bystrenova, Francesco Valle, and Fabio Biscarini*

CNR-Istituto per lo Studio dei Materiali Nanostrutturati (ISMN), Via Gobetti 101 - 40129 Bologna, Italy

Received: November 4, 2008; Revised Manuscript Received: January 24, 2009

The morphology of circular DNA deposited from a solution on the mica surface is analyzed from the power spectrum density (PSD) of the atomic force microscopy (AFM) images. Sample morphology is modulated in a broad range of concentration C from isolated molecules to highly entangled networks. DNA exhibits a multiaffine behavior with two correlation length scales: the persistence length P which remains constant (≈ 50 nm) within the C range and the intermolecular distance ξ which exhibits a decay with increasing C . Applying a diffusion based model in which ξ scales as $\xi \approx D^{-0.25} \cdot C^{-0.5}$, we extracted the DNA diffusion coefficient $D \approx 2 \times 10^{-7}$ cm²/s. This value is consistent with a high-molecular-weight plasmid DNA supercoiled in the solution.

Measurement of DNA morphological parameters has been a major issue in trying to understand the influence of surfaces on DNA morphology and functionality. It is particularly important in those systems where DNA is highly packed or forms entangled networks. Relevant examples include the cell genomic, where DNA takes with complex topologies and interacts with the quasi 2D cell surface;¹ the transcription and replication where knots and catenanes are formed;^{2,3} the DNA packing inside virus capsids which involves highly entangled topologies;⁴ the small circular DNA of bacteria which is usually present in very compact conformations (plectonemically supercoiled);⁵ the nanofabrication of nanostructures and patterned surfaces exploiting DNA self-assembly under conditions of high density.⁶

Morphology of DNA molecules has been extensively investigated by atomic force microscopy (AFM). One of the relevant morphological parameters extracted from AFM analyses is the persistence length (P), whose definition varies with the DNA model chosen.⁷ The worm-like chain model considers DNA as an intrinsically straight polymer partly relaxed by the effect of a thermal bath.⁸ Persistence length $P = YI/k_B T$ is the orientational correlation length along the chain expressed as a function of Young's modulus Y , the inertial moment I of the molecule, and the absolute temperature T ; k_B is the Boltzmann constant. The freely jointed chain model considers the polymer as a chain of independent segments of length $2P$ (termed as Kuhn segments) with no correlations.⁹ Independently of the model, P is a characteristic length of DNA that is a measure of its stiffness: the larger P , the more rigid is the polymer.⁹ P is used to assess the interaction of DNA with DNA binding molecules such as intercalating drugs¹⁰ or minor groove binding molecules,¹¹ and to characterize the effects of external DNA damaging factors such as UV light.¹²

Morphological DNA parameters are estimated by vectorization and analysis of individual DNA molecules from the AFM images, averaging on statistical sets of discrete elements. Proposed analyses of DNA morphology rely on the statistics

of the angles between vectors^{8,13} or on topological scaling properties.^{14,15} The former approach requires the choice of a model and dimensionality; the latter is model independent. Robustness of the data requires accumulation of large numbers of molecules, viz., many images or fewer images with a high density of molecules. As the density of molecules on the surface increases, singling out individual molecules becomes prohibitive as intermolecular contacts set on. Since the topology of DNA on surfaces implies always that a minority fraction of pixels are contributed by DNA, any image processing aimed to resolve the individual DNA molecules, mostly containing information in their contour, has to be carefully assessed. It would be desirable to perform a global analysis method on the whole AFM image without restriction on DNA surface density and, at the same time, without a specific assumption of an interpretative model.

In this Letter, we show that the power spectrum density (PSD) analysis of AFM images yields a robust value for P even at a high density of DNA molecules on the surface. The mean value of P is equivalent to that obtained by vectorization methods. PSD contains the information on the spatial distribution of DNA molecules on the surface across multiple length scales.¹⁶ This allows us to readily extract another characteristic length ξ which relates to the intermolecular distance of the DNA deposit. We show in fact that ξ scales with the DNA concentration, while P , as expected, is statistically invariant with respect to the amount of DNA on the surface. Our work demonstrates that the PSD analysis is a statistically robust and versatile method for the quantitative measurement of characteristic length scales of DNA morphology.

The PSD is the square norm of the Fourier transform of an AFM image, and represents the contribution of each spatial frequency to the topography.¹⁷ Owing to the isotropic features (in terms of molecular shape and in-plane orientation of the molecules) of our DNA samples, we used the one-dimensional PSD obtained by transforming the image line by line along the fast scan direction and averaging. As the analysis allows one to explore a range of frequencies ν between $\nu_{\min} = 1/L$ (L being

* To whom correspondence should be addressed. Phone: +39 051 639 85 22. Fax: +39 051 639 85 40. E-mail: f.biscarini@bo.ismn.cnr.it.

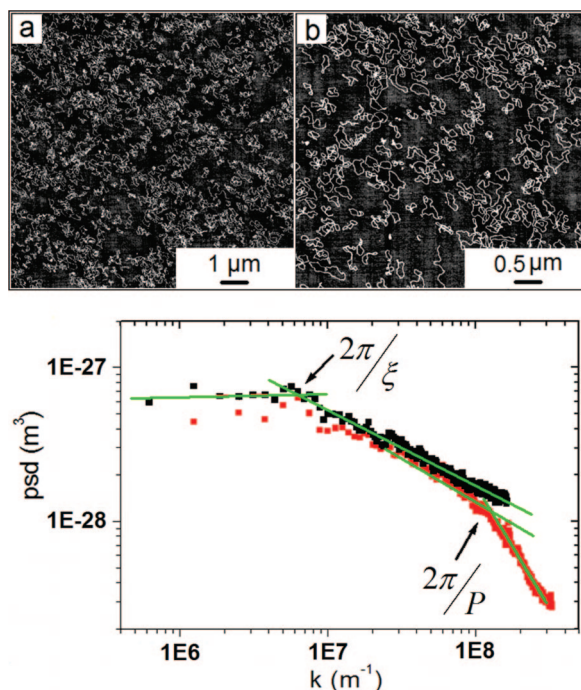


Figure 1. AFM images and their corresponding average power spectra for a sample obtained depositing DNA from a 0.75 $\mu\text{g/mL}$ solution. The scan area is (a) 10×10 and (b) $5 \times 5 \mu\text{m}^2$. The arrows point to the characteristic wave vectors, from which correlation lengths $\xi = 1 \mu\text{m}$ and $P = 50 \text{ nm}$ are extracted.

the image size) and the Nyquist frequency $\nu_{\text{max}} = N/(2L)$ (N being the number of pixels of the image),¹⁶ it is necessary to scan surfaces with an area lower than $5 \times 5 \mu\text{m}^2$ and a resolution of at least 512×512 pixels in order to access information on length scales in the order of a few tens of nanometers.

Samples were obtained by depositing DNA (pUC19 from *Escherichia coli* RR1, Sigma catalog nr. D3404, 2686 bp, MW = 1.8×10^6 Da) on muscovite mica from 10 μL UHQ aqueous solutions containing MgCl_2 in 5 mM concentration (DNA concentration in the range 0.375–1.5 $\mu\text{g/mL}$); the samples were washed and dried with pure nitrogen after 10 min. For each sample, at least five AFM images were acquired. For each image, the PSD analysis was performed on the raw data, after trend correction by line-by-line removal of the best-fit curve.

Figure 1 shows two images with different scan lengths and their corresponding PSDs, in double-log representation, vs spatial frequency represented as wave vector $k = 2\pi\nu$. Images were obtained on a sample from a 0.75 $\mu\text{g/mL}$ DNA solution. A large number of separated DNA molecules are visible. The PSDs exhibit a low-frequency plateau (white spectrum) followed by a frequency-decaying region, that we approximate by two power-law decays, each spanning about 1 order of magnitude of the spatial frequencies. The power-law decay indicates spatial correlations, and the characteristic frequencies where the different regions intersect are related to inverse correlation lengths. This behavior is termed multifractal.¹⁸ The larger correlation length (about 1 μm), which is the inverse of the smaller characteristic frequency, approximates the intermolecular distance. The smaller one (60 nm) matches the persistence length values reported in the literature.^{8,10,12,15} Smaller length scales, like the helix pitch and the DNA diameter, would contribute only to frequencies higher than $N/(2L)$ and are therefore not accessible.

We analyze a set of seven plasmid DNA samples with different densities of molecules on the surface. Figure 2 shows

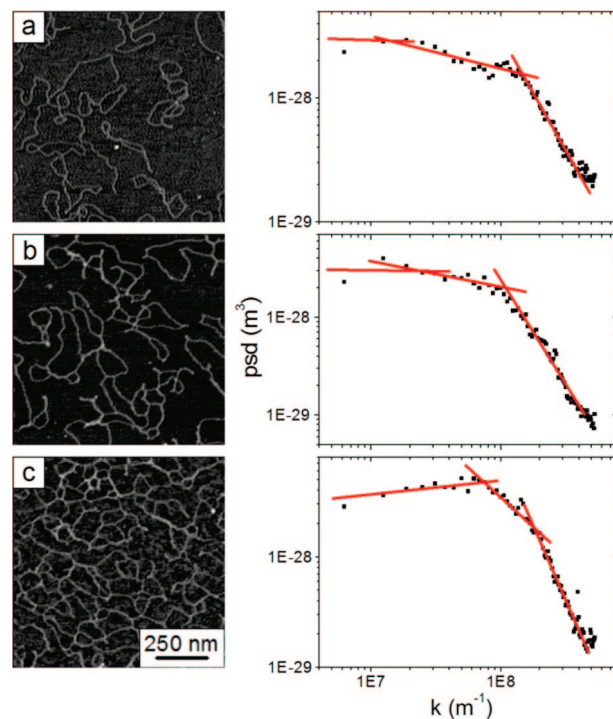


Figure 2. AFM images (left) of DNA deposited from solutions at different concentrations ((a) 0.375 $\mu\text{g/mL}$; (b) 1.05 $\mu\text{g/mL}$; (c) 1.5 $\mu\text{g/mL}$), and their corresponding power spectra (right). Continuous lines represent the fit to the white spectrum and decaying regions.

three AFM images at different DNA concentrations. In the range of concentration, the adsorption of DNA molecules changes from a diluted to highly entangled regime, characterized by the presence of overlapping strands. The analysis of the corresponding PSDs shows that the intersection between the two power-law-decaying portions of the PSD remains approximately constant. The intersection between the white spectrum region and the adjacent power-law-decaying portion instead shifts toward higher frequency values with increasing concentrations.

Figure 3 shows the evolution of the two correlation lengths as a function of DNA concentration C in the solution.

The smaller length scale P does not significantly change across the range of C (Figure 3a). The average value of P for all of the concentrations is $48 \pm 4 \text{ nm}$, which is consistent with the values reported in the literature for the persistence length.¹⁹ For comparison, the value of P ($52 \pm 20 \text{ nm}$) that we obtained upon a statistical analysis of the angular correlation decay by vectorization of the individual DNA molecules is shown.⁸ The vectorization is suitable for the lower limit of the concentration range explored in this work, whereas the PSD analysis applies to the whole range from very diluted to highly entangled DNA at the surface.

The larger length scale ξ exhibits a decaying trend vs C (Figure 3b). To discuss this, we assume that the diffusion of DNA molecules from the solution to the surface is the process determining the adsorption rate of DNA on the surface. According to ref 20, the density n_s of DNA molecules on the surface is related to the concentration C as

$$n_s = \frac{CN_A}{MW} \cdot \sqrt{\frac{4Dt}{\pi}} \quad (1)$$

where D is the diffusion coefficient of DNA, N_A is Avogadro's number, MW the DNA molecular weight, and the time t is kept constant in our experiment (10 min).

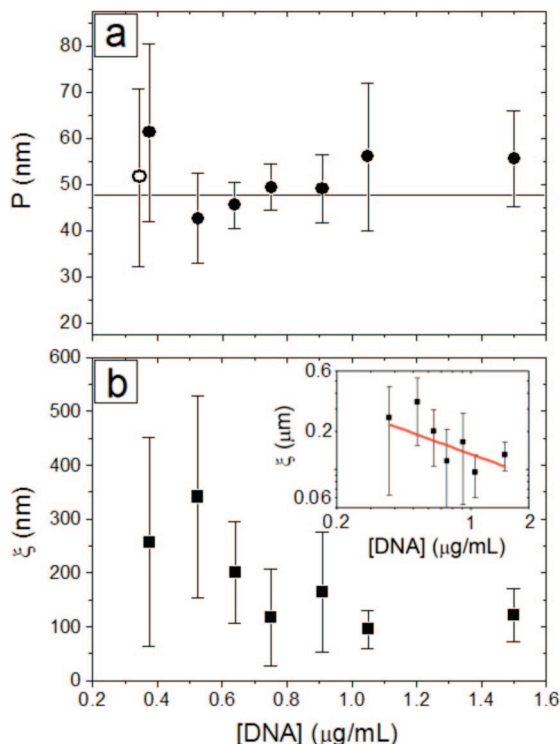


Figure 3. (a) Evolution of persistence length versus DNA concentration C . The average value is 48 ± 4 nm. The persistence length extracted from a statistical set of 64 molecules at concentration $0.375 \mu\text{g/mL}$ according to the method in ref 8 yields $P = 52 \pm 20$ nm (open circle). (b) Evolution of the intermolecular distance ξ vs C . The inset shows the power-law fit according to eq 3 in double-log scale.

We assume that the area available for a single DNA molecule is approximately equal to ξ^2 ,²¹ to obtain

$$\frac{1}{\xi^2} \approx n_s = \frac{CN_A}{MW} \cdot \sqrt{\frac{4Dt}{\pi}} \quad (2)$$

Consequently, we expect the dependence of ξ vs C to be a power law:

$$\xi = \xi_0 C^{-1/2} \quad (3)$$

where ξ_0 is a function of the diffusion coefficient D as

$$\xi_0 = \left(\frac{MW}{N_A}\right)^{1/2} \cdot \left(\frac{\pi}{4Dt}\right)^{1/4} \quad (4)$$

We fit the experimental data of ξ with the power law of eq 3 (using the error bars as statistical weights), obtaining $\xi_0 = (1.5 \pm 0.16) \times 10^{-8} (\text{g/cm})^{1/2}$. A fit with the exponent in eq 3 free, yields a best-fit exponent of -0.55 ± 0.34 and $\xi_0 = (1.32 \pm 0.16) \times 10^{-8} (\text{g/cm})^{1/2}$. From eq 4, we extract $D = (2.3 \pm 1) \times 10^{-7} \text{ cm}^2/\text{s}$. This value can be compared to the value $(5.4 \pm 0.2) \times 10^{-8} \text{ cm}^2/\text{s}$ in ref 8 upon introducing the phenomenological correction for the different molecular weight:

$$D_{\text{pUC19}} = D_{\text{ref8}} \cdot (MW_{\text{pUC19}}/MW_{\text{ref8}})^{0.571} \cdot f \quad (5)$$

The ratio of molecular weights comes from Flory's law, and f is a phenomenological factor which accounts for the plasmid conformation ($f = 1.6$ – 1.8 for supercoiled plasmids, $f = 1.3$ for relaxed plasmids).²² Our value is consistent if $f = 2.8 \pm 1.2$, which suggests that our DNA plasmid is supercoiled in the solution.

These results are in good agreement with the fact that the DNA population extracted from bacteria—as pUC19—is composed mainly by supercoiled plasmids. Our value is 1 order of magnitude larger than the value for supercoiled pUC19 from earlier dynamic light scattering measurements.²³ However, the latter value was affected by contamination of plasmid dimers and trimers which leads to an underestimation of the diffusion coefficient. The consistency of our data with the diffusion model also confirms that we can identify ξ as the characteristic distance of the area occupied by a single DNA molecule.

In conclusion, we presented a method based on the spectral analysis on AFM images which accounts for all of the molecules present in the image, without requiring either model assumptions, molecule sorting, or operator-biased processing. The method is completely general, and can be applied to the investigation of the morphological effects related to a variety of experimental parameters, e.g., ionic strength, temperature, surfactant and surface interactions. In the case examined here, where we change systematically the concentration of the depositing DNA solution, we showed that two characteristic lengths of DNA topology, viz., intermolecular distance and persistence length, can be extracted. One of the main advantages is that the analysis can be applied to the case of high DNA coverage, where it is not possible to single out the molecules due to the large number of contacts, as well as in the presence of very coiled DNA where vectorization becomes prohibitive. We show that the scaling of the intermolecular distance is consistent with a deposition governed by diffusion and allows a value for the diffusion coefficient of the plasmid DNA to be extracted.

The PSD method provides new insights on DNA topology, as the presence of multiaffine behavior. This is symptomatic of the hierarchical organization of DNA on the surface. Its detailed analysis can open interesting perspectives on the study of the mechanism of interaction between DNA and the surface environment, as well as on its structure–functionality correlation.

Acknowledgment. This work was supported by EU contract NMP BIODOT. A.C. acknowledges INSTM fellowship under EU project STAG; P.S. is supported by ESF EURYI DYMUT.

References and Notes

- (1) Hetzer, M. W.; Walther, T. C.; Mattaj, I. W. *Annu. Rev. Cell. Dev. Biol.* **2005**, *21*, 347.
- (2) Olavarrieta, L.; Martinez-Robles, M. L.; Hernandez, P.; Krimer, D. B.; Schwartzman, J. B. *Mol. Microbiol.* **2002**, *46*, 699.
- (3) Olavarrieta, L.; Martinez-Robles, M. L.; Sogo, J. M.; Stasiak, A.; Hernandez, P.; Krimer, D. B.; Schwartzman, J. B. *Nucleic Acids Res.* **2002**, *30*, 656.
- (4) Arsuaga, J.; Vazquez, M.; McGuirk, P.; Trigueros, S.; Summers, D. W.; Roca, J. *Proc. Natl. Acad. Sci. U.S.A.* **2005**, *102*, 9165.
- (5) Pope, L. H.; Davies, M. C.; Laughton, C. A.; Roberts, C. J.; Tendler, S. J.; Williams, P. M. *J. Microsc.* **2000**, *199*, 68.
- (6) Xiao, Z. W.; Xu, M. X.; Ohgi, T.; Sagisaka, K.; Fujita, D. *Superlattices Microstruct.* **2002**, *32*, 215.
- (7) Ullner, M.; Woodward, C. E. *Macromolecules* **2002**, *35*, 1437.
- (8) Rivetti, C.; Guthold, M.; Bustamante, C. *J. Mol. Biol.* **1996**, *264*, 919.
- (9) Dill, K.; Bromberg, S. *Molecular Driving Forces - Statistical Thermodynamics in Chemistry and Biology*; Garland Science: New York, NY, 2003; Vol. 1, Chapter 32, p 609.
- (10) Berge, T.; Jenkins, N. S.; Hopkirk, R. B.; Waring, M. J.; Edwardson, J. M.; Henderson, R. M. *Nucleic Acids Res.* **2002**, *30*, 2980.

- (11) Reddy, B. S. P.; Sharma, S. K.; Lown, J. W. *Curr. Med. Chem.* **2001**, 8, 475.
- (12) Lysetska, M.; Knoll, A.; Boehringer, D.; Hey, T.; Krauss, G.; Krausch, G. *Nucleic Acids Res.* **2002**, 30, 2686.
- (13) Rivetti, C.; Walker, C.; Bustamante, C. *J. Mol. Biol.* **1998**, 280, 41.
- (14) Ercolini, E.; Valle, F.; Adamcik, J.; Witz, G.; Metzler, R.; De Los Rios, P.; Roca, J.; Dietler, G. *Phys. Rev. Lett.* **2007**, 98, 058102.
- (15) Valle, F.; Favre, M.; De Los Rios, P.; Rosa, A.; Dietler, G. *Phys. Rev. Lett.* **2005**, 95, 158105.
- (16) Biscarini, F.; Samorì, P.; Greco, O.; Zamboni, R. *Phys. Rev. Lett.* **1997**, 78, 2389.
- (17) Jenkins, W. K. In *Digital Signal Processing Handbook CRCnet-BASE*; Madisetti, V. K.; CRC press LLC: Boca Raton, FL, 1999; Vol. 1, Chapter 1, p 12.
- (18) Barabasi, A.-L.; Stanley, H. E. *Fractal concepts in surface growth*; Cambridge University Press: Cambridge, UK, 1995; Vol. 1, Chapter 3, p 36.
- (19) Bustamante, C.; Marko, J. F.; Siggia, E. D.; Smith, S. *Science* **1994**, 265, 1599.
- (20) Lang, D.; Coates, P. *J. Mol. Biol.* **1968**, 36, 137.
- (21) The equality ξ in eq 2 implies that a Euclidean partition of the surface can be made, which holds when the surface coverage by self-affine DNA molecules is low and they are distant apart. At high concentration and entangled networks, the surface is paved with self-affine (in 2D) objects, and a substantial deviation from the density scaling ξ should be expected. As the density of molecules increases, ξ approaches the effective diameter of the DNA molecule and the scaling of eq 2 becomes $1/\xi^{d_f} \approx a(CN_A/MW)(4Dt/\pi)^{1/2}$, where the fractal dimension d_f takes a value between 1 and 2 and the constant a accounts for the dimensional consistency.
- (22) Robertson, R. M.; Laib, S.; Smith, D. E. *Proc. Natl. Acad. Sci. U.S.A.* **2006**, 103, 7310.
- (23) Fishman, D. M.; Patterson, G. D. *Biopolymers* **1995**, 38, 535.

JP8097318